Int. J. Appl. Math. Comput. Sci., 2023, Vol. 33, No. 1, 71–82
DOI: 10.34768/amcs-2023-0006

ON THE FINITE TIME STABILIZATION VIA ROBUST CONTROL FOR UNCERTAIN DISTURBED SYSTEMS

PATRICIO ORDAZ [a,*], HUSSAIN ALAZKI [b], BONIFACIO SÁNCHEZ [a,c], MARIO ORDAZ-OLIVER [c]

[a] Institute of Basic Sciences and Engineering
Autonomous University of Hidalgo State
Carretera Pachuca-Tulancingo Km. 4.5, Colonia Carboneras, 42184, Mineral de la Reforma, Hidalgo, Mexico
e-mail: jesus_ordaz@uaeh.edu.mx

[b] Faculty of Engineering
Autonomous University of Carmen
Av. 56 No. 4, Esq. Avenida Concordia Col. Benito Juárez, 24180, Ciudad del Carmen, Campeche, Mexico

[c] School of Engineering
La Salle University
Av. San Juan Bautista de la Salle, 1, San Juan Tilcuautla, 42160, Hidalgo, Mexico

This paper deals with the finite-time stabilization problem for a class of uncertain disturbed systems using linear robust control. The proposed algorithm is designed to provide the robustness of a linear feedback control scheme such that system trajectories arrive at a small-size attractive set around an unstable equilibrium in a finite time. To this end, an optimization problem with a linear matrix inequality constraint is presented. This means that the effects of external disturbances, as well as matched and mismatched uncertain dynamics, can be significantly reduced. Finally, the performance of the suggested closed-loop control strategies is shown by the trajectory tracking of an unmanned aerial vehicle flight.

Keywords: finite time bounded stability, uncertain disturbed systems, robust stabilization, ultimate bound minimization.

1. Introduction

The control of dynamic systems in practice is complex, mainly because the effects of external disturbances as well as unknown dynamical phenomena cannot be neutralized (Amato *et al.*, 2014; Edwards and Spurgeon, 1998). Trajectories of controlled systems do not converge to a known fixed point for the stabilization problem when this phenomenon is latent. However, the uncertain-disturbed system's trajectory can arrive in a region of attraction around the origin or a known fixed point (Bhat and Bernstein, 2000; Haddad and Chellaboina, 2011; Khalil and Grizzle, 2002; Poznyak *et al.*, 2014; Kukurowski *et al.*, 2022). Indeed, an acceptable control law for a control system may cause the system's trajectory to go around the origin. Furthermore, this has the effect of reducing the size of the region of attraction as well as attenuating the uncertain-disturbance effect. If this occurs in a finite time, then it is associated with the so-called finite-time bounded (FTB) stability (Amato *et al.*, 2014; 2001; Bhat and Bernstein, 2000). This notion can now be connected to certain robust controllers. Control strategies based on linear matrix inequalities (LMI), attractive ellipsoid method (AEM), $\mathcal{H}_\infty$ robust control, sliding mode control (SMC) are only a few examples (Amato *et al.*, 2001; Edwards and Spurgeon, 1998; Kokotović *et al.*, 2006; Poznyak *et al.*, 2014; Liu *et al.*, 2018).

The idea of finite-time stability is related to a set of necessary and sufficient conditions that may be investigated from many angles (Amato *et al.*, 2003; Bhat and Bernstein, 2000; Li *et al.*, 2019). The case of FTB stability for a class of linear disturbed systems was provided by applying the notion of convex optimization (Amato *et al.*, 2003). Thus, by including the constraint matrix inequality problem in the system stability analysis,

*Corresponding author

the notion of FTB-stability may be successfully applied (Amato *et al.*, 2003; 2001; Kokotović *et al.*, 2006; Polyakov *et al.*, 2015; Puangmalai *et al.*, 2020; Yu *et al.*, 2005).

On the other hand, the theory of finite-time stability of continuous autonomous systems was introduced by Bhat and Bernstein (2000) by satisfying some Lyapunov and converse Lyapunov scalar differential inequalities. Naturally, this research is focused on FTB stability for uncertain-disturbed systems. To provide robust control, properties of sliding-mode control based on the Lyapunov method are combined with finite-time and practical stability concepts (Edwards and Spurgeon, 1998; Li *et al.*, 2019; Orlov *et al.*, 2010; Yu *et al.*, 2005).

As previously stated, the idea of FTB stability is closely related to the problem of stabilizing control systems that are susceptible to uncertainties and external disturbances (Amato *et al.*, 2003; Kokotović *et al.*, 2006; Polyakov *et al.*, 2015). Uncertainties and external disturbances can degrade the system trajectory behavior and, in certain situations, cause control system instability (Haddad and Chellaboina, 2011; Khalil and Grizzle, 2002; Kokotović *et al.*, 2006). The problem is concerned with reducing the effects of this phenomenon in the case of high precision on control systems vulnerable to uncertainties and/or external disturbances. In reality, the difficulty of completely avoiding the effects of unmatched external disturbances as well as uncertain dynamics in single or multiple input-multiple output systems is still an open problem.

Today, certain robust controllers have been created to mitigate the consequences of mismatched disturbances (Amato *et al.*, 2001; Edwards and Spurgeon, 1998; Kokotović *et al.*, 2006; Poznyak *et al.*, 2014). This includes everything from conventional controller development and implementation to sophisticated controllers in a variety of structured variables, adaptive schemes, and neuro-fuzzy processes, among others (Edwards and Spurgeon, 1998; Utkin and Poznyak, 2013; Wang *et al.*, 2019).

In this paper, linear feedback robust control is used to improve the trajectory performance of as class of uncertain disturbed system. To this end, the system under consideration was subdivided into matched uncertain-disturbed dynamics and unmatched uncertain-disturbed dynamics. In this sense, the robust control is therefore designed by introducing an adjoint manifold and employing the Cauchy–Schwarz inequality. Actually, an optimization problem subject to a certain linear matrix inequality was supplied to carry the system trajectory around the origin. In this sense, the main contribution lies in the linear robust control design for a class of nonlinear systems. In addition, a sufficient condition to conclude with FTB stability of a closed-loop system with a small attraction region is presented.

The paper outline is as follows. Section 2 presents the mathematical background, system description, and problem statement. In Section 3, the main result dealing with the robust control design for a class of uncertain disturbed systems is presented. Theoretical results are validated in Section 4, where an illustrative example, dealing with the stabilization of unmanned aerial vehicle systems and a brief comparative study is presented. Finally, concluding remarks are exposed in Section 5.

2. Preliminaries and problem formulation

Consider the uncertain and disturbed control system

$$\dot{x}(t) = f(x(t)) + \mathbf{B}u(t) + d(t), \;\; x(0) = x_0, \tag{1}$$

where $x \in D \subset \mathbb{R}^n$ is a connected manifold at time $t \geq 0$, the nonlinear function $f : \mathbb{R}^n \to \mathbb{R}^n$ fulfills the trivial solution $f(0) = 0$, and it may contain parameter or dynamic uncertainty. The admissible control input is given by $u \in \mathcal{U} \subset \mathbb{R}^m$, and $\mathbf{B}$ is a known real constant matrix with appropriate dimensions. The external non-vanishing disturbance effects are denoted by $d \in \mathbb{R}^n$. Notice that the uncertain disturbed system (1) can also be expressed as

$$\begin{aligned} \dot{x}(t) &= \mathbf{A}x(t) + \mathbf{B}u(t) + \xi(x,t), \quad x(0) = x_0, \\ \xi(x,t) &= f(x(t)) - \mathbf{A}x(t) + \mathbf{B}\xi_u(t) + d(t), \end{aligned} \tag{2}$$

where $\mathbf{A}$ is an $n \times n$ matrix associated with the linear form of the nonlinear vector function f. Nonlinear dynamics, system uncertainties and external disturbances are denoted as ξ. In fact, $\xi_u \in \mathbb{R}^m$ and $d \in \mathbb{R}^n$ define the matched and unmatched system uncertainties and external disturbances, respectively. Actually, ξ contains high order terms after linearization of the nonlinear vector function f and/or external disturbances.

Before the problem formulation, the following assumptions are made.

Assumption 1. The nonlinear dynamic, system uncertainties and external disturbances are assumed to be bounded as $\|\xi(x,t)\| \leq \delta < \infty$, at least locally. Furthermore, ξ is a class of unmatched and matched uncertainties and disturbances.

Assumption 2. The nominal system (2) is controllable to the equilibrium solution. From the above it follows that the pair $(\mathbf{A}, \mathbf{B})$ is controllable too.

The transformation $z = \mathbf{T}x$ is used to describe a regular form, where $\mathbf{T} \in \mathbb{R}^{n\times n}$ is defined by[1]

$$\mathbf{T} = \begin{bmatrix} \mathbf{N_B} & \mathbf{B} \end{bmatrix}^\top, \tag{3}$$

where the matrix $\mathbf{N_B} \in \mathbb{R}^{m\times(n-m)}$ represents a basis of the null-space of $\mathbf{B}^\top$.

[1]For single input systems, the similarity transformation to a controllable canonical form may be used.

Consequently, it is evident that system (2) can be represented as

$$\begin{bmatrix}\dot z_1(t)\\ \dot z_2(t)\end{bmatrix} = \begin{bmatrix}\boldsymbol{\mathcal{A}}_{11} & \boldsymbol{\mathcal{A}}_{12}\\ \boldsymbol{\mathcal{A}}_{21} & \boldsymbol{\mathcal{A}}_{22}\end{bmatrix}\begin{bmatrix}z_1(t)\\ z_2(t)\end{bmatrix} + \begin{bmatrix}\boldsymbol{\mathcal{B}}_1\\ \boldsymbol{\mathcal{B}}_2\end{bmatrix} u + \begin{bmatrix}\bar\xi_1(x,t)\\ \bar\xi_2(x,t)\end{bmatrix}, \tag{4}$$

$$\begin{aligned} \boldsymbol{\mathcal{A}} &= \mathbf{TAT}^{-1}, \quad \boldsymbol{\mathcal{B}} = \mathbf{TB},\\ \bar\xi &= \mathbf{T}\xi(z,t), \quad \boldsymbol{\mathcal{B}}_1 = \mathbf{0}_{(n-m)\times m},\\ z_1(0) &= z_{01}, \qquad z_2(0) = z_{02}, \end{aligned}$$

where $z_1 \in \mathbb{R}^{n-m}$, $z_2 \in \mathbb{R}^m$, the matrices $\boldsymbol{\mathcal{A}}_{11}$, $\boldsymbol{\mathcal{A}}_{12}$, $\boldsymbol{\mathcal{A}}_{21}$, $\boldsymbol{\mathcal{A}}_{22}$, having appropriate dimensions. On the assumption that the rank of $\mathbf{B}$ is m, it follows that $\boldsymbol{\mathcal{B}}_2 = \mathbf{B}^\top\mathbf{B}$, so that $\boldsymbol{\mathcal{B}}_2 \in \mathbb{R}^{m\times m}$ is nonsingular.

Assumption 3. The system transformation satisfies the condition

$$\|\bar\xi_1(t)\| \le \delta_1, \quad \|\bar\xi_2(t)\| \le \delta_2, \tag{5}$$

where $0 < \delta_1 < \infty$, $0 < \delta_2 < \infty$, and $\|\cdot\|$ denotes the standard Euclidean norm.

Problem statement. The aim is to provide an algorithm to obtain the matrix gain $\mathbf{K}$ for an admissible control signal

$$u = \mathbf{K}x, \quad \mathbf{K} \in \mathbb{R}^{m\times n}, \tag{6}$$

such that the effects of nonvanishing uncertainties and disturbances are considerably reduced. Actually, the main objective is to guarantee that, in a closed loop with (6), the trajectory of system (2) arrives at an attractive set $\Omega = \{x \in \mathbb{R}^n : \|x\| \le \varkappa\}$ in a finite time $T_r = t_0 + T$ for $\varkappa \in \mathbb{R}^+$ as small as possible.

Theorem 1. (Cauchy–Schwarz inequality (Edwards and Spurgeon, 1998; Poznyak *et al.*, 2014)) *Let y and w be two vectors in $\mathbb{R}^n$. Then we have $\langle y, w\rangle^2 \le \|y\|^2\|w\|^2$, or equivalently $|\langle y, w\rangle| \le \|y\|\|w\|$, where $\langle\cdot,\cdot\rangle$ denotes the inner or dot product between two vectors.*

Definition 1. (*Finite-time bounded stability (Weiss and Infante, 1967; Amato* et al.*, 2014)*) The nonlinear system, $\dot x = f(x,t) + \xi(x,t)$, is said to be stable under perturbing forces, or finite-time bounded (FTB), with respect to positive real numbers (a, b, ϵ, T) if

$$\|x(t_0)\| < a \text{ and } \xi(x,t) \le \epsilon \implies \|x(t)\| \le b,$$

for all time instants $t \ge t_0 + T$.

The previous definition can be associated with a positive definite function $V : D \to \mathbb{R}$ defined in a domain $D \subset \mathbb{R}^n$ that contains the origin.

Lemma 1. *Let the function $V : \mathbb{R}^n \to \mathbb{R}$ satisfy*

$$\frac{\mathrm{d}}{\mathrm{d}t}V(t) + \alpha V(t) \le \beta\sqrt{V(t)}, \quad V(t_0) = V_0. \tag{7}$$

Then, for any initial condition V_0, positive scalars α and β, the solution $V(t)$ is stable in the FTB-sense, with

$$T = \frac{2}{\alpha}\ln\left\{\frac{\alpha V(t_0) - 2\beta}{\alpha\gamma}\right\} + t_0, \tag{8}$$

for a sufficiently small $\gamma < 0$ and bound $b = 2\beta/\alpha + \gamma$.

Lemma 2. *Let the function V satisfy*

$$\frac{\mathrm{d}}{\mathrm{d}t}V(t) + \alpha V(t) \le \beta, \quad V(t_0) = V_0. \tag{9}$$

Then, for positive scalars α and β, the storage function $V(t)$ is stable in the FTB-sense, with

$$b = \frac{\beta + \alpha\gamma}{\alpha}, \quad T = \frac{1}{\alpha}\ln\left\{\frac{\alpha V(t_0) - \beta}{\beta\gamma}\right\} + t_0, \tag{10}$$

for a sufficiently small positive scalar γ.

3. Main contribution

In order to reduce the effects of $\bar\xi$ in (4), consider the adjoint system variable $\varphi : \mathbb{R}^m \times \mathbb{R}^{n-m} \to \mathbb{R}^m$ as

$$\varphi = z_2 + \mathbf{R}_1 z_1, \quad \mathbf{R}_1 \in \mathbb{R}^{m\times(n-m)}, \tag{11}$$

where $\mathbf{R}_1$ is an adjustment matrix. Thus, by enclosing the variable φ into an invariant set $\Omega = \{\varphi \in \mathbb{R}^m : \|\varphi\| \le \delta\}$, for δ small enough, such effects must be considerably reduced.

Proposition 1. *For a fixed matrix gain $\mathbf{R}_1$, assume that the matrix gain $\boldsymbol{\mathcal{K}} \in \mathbb{R}^{n\times m}$ of a linear control action $u = \boldsymbol{\mathcal{K}}z$, associated system* (4)*, is given by*

$$\begin{aligned} \boldsymbol{\mathcal{K}} &= -\boldsymbol{\mathcal{B}}_2^{-1}\left[\boldsymbol{\mathcal{K}}_1,\ \boldsymbol{\mathcal{K}}_2\right],\\ \boldsymbol{\mathcal{K}}_1 &= \boldsymbol{\mathcal{A}}_{21} + \mathbf{R}_1\boldsymbol{\mathcal{A}}_{11} + \mathbf{R}_2^2\mathbf{R}_1,\\ \boldsymbol{\mathcal{K}}_2 &= \boldsymbol{\mathcal{A}}_{22} + \mathbf{R}_1\boldsymbol{\mathcal{A}}_{12} + \mathbf{R}_2, \end{aligned} \tag{12}$$

where $\mathbf{R}_2 \in \mathbb{R}^{m\times m}$ is a diagonal positive definite adjustment matrix. Then the trajectory $\varphi(t)$ is FTB-stable, with arriving time

$$T_1 = \frac{2}{\alpha_1}\ln\left\{\frac{\alpha_1\|\varphi_0\| - 2\sqrt{2}\beta_1}{\alpha_1\gamma_1}\right\} + t_0, \tag{13}$$

around the set $\Omega_1 = \{\varphi \in \mathbb{R}^m : \|\varphi\| \le b_1\}$, where $b_1 = \sqrt{2}\beta_1/\alpha_1 + \gamma_1$, for a sufficiently small positive scalar γ_1, positive numbers

$$\alpha_1 = \lambda_{\min}(\mathbf{R}_2)$$

and

$$\beta_1 = 2\sqrt{\delta_2^2 + \lambda_{\max}(\mathbf{R}_1^\intercal\mathbf{R}_1)\delta_1}.$$

Finally, in order to use the control law (12) on system (2), the inverse transformation $x = \mathbf{T}^{-1}z$ must be applied. In this sense, the control law

$$u = \mathbf{K}x, \quad \mathbf{K} = -\boldsymbol{\mathcal{B}}_2^{-1}\left[\boldsymbol{\mathcal{K}}_1,\ \boldsymbol{\mathcal{K}}_2\right]\mathbf{T} \tag{14}$$

is concluded.

The zone of attraction of φ is defined by the previous statement, and the size of the region is determined by known parameters δ_1, δ_2 and adjustment gain matrices $\mathbf{R}_1, \mathbf{R}_2$.

Remark 1. Assume that Proposition 1 is fulfilled. Using Lemma 1, it is evident that if the initial condition φ_0 starts within the set Ω_1, this one remains in there for all future time. Actually, a sufficiently large α_1 implies a small size attractive set Ω_1.

After time T_1, the adjoint variable $\varphi = z_2 + \mathbf{R}_1 z_1$ leads to

$$z_2 = \varphi - \mathbf{R}_1 z_1, \quad \|\varphi\| \leq \frac{\sqrt{2}\beta_1}{\alpha_1} + \gamma_1. \tag{15}$$

Furthermore, the previous result implies that the dynamics of z_1, from (4), are

$$\begin{aligned} \dot{z}_1 &= \left(\boldsymbol{\mathcal{A}}_{11} - \boldsymbol{\mathcal{A}}_{12}\mathbf{R}_1\right) z_1 + \bar{\varphi}(t), \\ \bar{\varphi}(t) &= \boldsymbol{\mathcal{A}}_{12}\varphi(t) + \bar{\xi}_1(z,t), \quad z_1(0) = z_1^0. \end{aligned} \tag{16}$$

Proposition 1 works by considering the knowledge of gain matrix $\boldsymbol{\mathcal{K}}$, but this matrix may provoke system stability or instability. Therefore, the adequate design $\boldsymbol{\mathcal{K}}$ is required in order to guarantee stability of system (4).

Proposition 2. *Let the assumptions Proposition 1 be met. After time $t \geq T_1$, if there exists a solution set $(\alpha_2, \varepsilon_1, \varepsilon_2, \mathbf{P}, \mathbf{R}_1)$, where $0 < \mathbf{P}^\top = \mathbf{P} \in \mathbb{R}^{(n-m)\times(n-m)}$, $\mathbf{R}_1 \in \mathbb{R}^{m\times(n-m)}$ are adjustment matrices, positive scalars α_2, ε_1 and ε_2, such that the following matrix inequality is fulfilled:*

$$\mathbf{W} = \begin{bmatrix} \mathbf{PF} + \mathbf{F}^\intercal\mathbf{P} + \alpha_2\mathbf{P} & \mathbf{P} & \mathbf{P}\boldsymbol{\mathcal{A}}_{12} \\ \mathbf{P} & -\varepsilon_1\mathbf{I}_{n-m} & \mathbf{0}_{(n-m)\times m} \\ \boldsymbol{\mathcal{A}}_{12}^\intercal\mathbf{P} & \mathbf{0}_{m\times(n-m)} & -\varepsilon_1\mathbf{I}_m \end{bmatrix} < 0,$$

$$\mathbf{F} = \boldsymbol{\mathcal{A}}_{11} - \mathbf{R}_1\boldsymbol{\mathcal{A}}_{12}, \tag{17}$$

then the trajectory $z_1(t)$ of system (4) is stable in the FTB-sense, with $\beta_2 = \varepsilon_1\delta_1 + \varepsilon_2\delta_2$, positive fixed scalar α_2 and

$$\begin{aligned} b_2 &= \sqrt{\frac{\beta_2}{\alpha_2}\lambda_{\max}(\mathbf{P^{-1}})}, \\ T_2 &= \tfrac{1}{\alpha_2}\ln\left\{\frac{\alpha_2\lambda_{\max}(\mathbf{P})\|z_{01}\|^2 - \beta_2}{\alpha_2\gamma_2}\right\} + T_1, \end{aligned} \tag{18}$$

for a sufficiently small constant $\gamma_2 \in \mathbb{R}^+$.

The previous proposition is one way to obtain the gain matrix $\boldsymbol{\mathcal{K}}$ such that (16) is stable.

Remark 2. For system (16), note that $\boldsymbol{\mathcal{A}}_{12}$ plays the role of a related matrix input and $\mathbf{R}_1 z_1$ as its control input. Therefore, (16) can be rewritten as

$$\begin{aligned} &\dot{\bar{x}} = \bar{\boldsymbol{\mathcal{A}}}z_1 + \bar{\boldsymbol{\mathcal{B}}}\bar{u} + \bar{\varphi}(t), \quad \bar{x} = z_1, \\ &\bar{\boldsymbol{\mathcal{A}}} = \boldsymbol{\mathcal{A}}_{11},\ \bar{\boldsymbol{\mathcal{B}}} = -\boldsymbol{\mathcal{A}}_{12}, \quad \bar{u} = \bar{\boldsymbol{\mathcal{K}}}\bar{x}, \quad \bar{\boldsymbol{\mathcal{K}}} = \mathbf{R}_1. \end{aligned} \tag{19}$$

Thus, under the considered system dynamics, the coordinate transformation given by (3) can be applied to (19). Proposition 1 can be employed to guarantee the stability of z_1 in the FTB-sense. In fact, this procedure may be used recursively across all subsystems to reduce the effects of mismatched uncertain dynamics and external disturbances.

Corollary 1. *Let the assumptions of Propositions 1 and 2 be met. The system trajectory arrives into the attractive set*

$$\begin{aligned} \Omega = \{x \in \mathbb{R}^n : \|x\| \leq \varkappa\}, \quad \varkappa = \rho\sqrt{\lambda_{\min}(\mathbf{T}^{-1})}, \\ \rho = \sqrt{\left(b_1 + b_2\lambda_{\min}(\mathbf{R}_1^\top\mathbf{R}_1)^{\frac{1}{2}}\right)^2 + b_1^2}, \end{aligned} \tag{20}$$

in finite time T_2.

To obtain a reduced-size attractive set Ω with $\varkappa > 0$ as small as possible, it is sufficient to reduce the size b_2. Thus, the following constrained optimization problem is introduced:

$$\min_{\mathbf{P^{-1}}}\left(\frac{\beta_2}{\alpha_2}\lambda_{\max}(\mathbf{P^{-1}})\right) \tag{21a}$$

subject to

$$0 < \alpha_2, \quad 0 < \varepsilon_1, \quad 0 < \varepsilon_2, \quad 0 < \mathbf{P}, \quad \mathbf{W} < 0. \tag{21b}$$

Notice that the optimization problem (21b) is nonlinear. In order to convert it into an isomorphic linear one, the next result is provided.

Lemma 3. *Solution of* (21b) *is equivalent to solving the optimization problem*

$$\min_{\mathbf{X}} \frac{\beta_2}{\alpha_2}\mathrm{trace}(\mathbf{X}) \tag{22a}$$

subject to

$$0 < \alpha_2, \quad 0 < \varepsilon_1, \quad 0 < \varepsilon_2, \quad 0 < \mathcal{W}, \quad 0 < \mathbf{X}, \tag{22b}$$

where

$$\mathcal{W} = \begin{bmatrix} \mathcal{A}_{11}\mathbf{X} + \mathbf{X}\mathcal{A}_{11}^\intercal - \mathcal{A}_{12}\mathbf{Y} - \mathbf{Y}\mathcal{A}_{12}^\intercal - \alpha_2\mathbf{X} & -\mathbf{I} & -\mathcal{A}_{12} \\ -\mathbf{I} & \varepsilon_1\mathbf{I} & \mathbf{0} \\ -\mathcal{A}_{12}^\intercal & \mathbf{0} & \varepsilon_1\mathbf{I} \end{bmatrix}, \tag{23}$$

and the matrix gain of (16) *is given by $\mathbf{R}_1 = \mathbf{X}^{-1}\mathbf{Y}$.*

The following iterative procedure, provides a numerical solution to the optimization problem (22b):

1) First, fix some initial values $i = 0$, $j = 0$, $k = 0$, $0 < \varkappa_1 \ll 1$, $0 < \alpha_1 \ll 1$, $0 \ll \varepsilon_1$ and $0 \ll \varepsilon_2$. Apply the MATLAB Toolbox Yalmip-CVX to obtain the solution ($\mathcal{W}$, $\boldsymbol{\mathcal{X}}$ and $\boldsymbol{\mathcal{Y}}$) of the constrained optimization problem (22b).

2) Increase $i = i+1$, decrease α_1 as $\alpha_1 = \alpha_1 - i \times \varkappa_1$ and make sure that the problem (22b) is feasible under this new α. If this is the case, define $\mathcal{W} = \mathcal{W}_{i,j,k}$, $\boldsymbol{\mathcal{X}} = \boldsymbol{\mathcal{X}}_{i,j,k}$, $\boldsymbol{\mathcal{Y}} = \boldsymbol{\mathcal{Y}}_{i,j,k}$.

2.1) Increment $j = j + 1$, and update ε_1 as $\varepsilon_1 = \varepsilon_1 + j \times \varkappa_1$. Verify if the convex problem (22b) is feasible; if this is the case, execute the next loop:

2.2.1) Increment $k = k + 1$, and upload ε_2 as $\varepsilon_1 = \varepsilon_1 + k \times \varkappa_1$. Verify that convex problem (22b) is feasible.

2.2.2) If this is the case, store the solution as $\mathcal{W} = \mathcal{W}_{i,j,k}$, $\boldsymbol{\mathcal{X}} = \boldsymbol{\mathcal{X}}_{i,j,k}$, $\boldsymbol{\mathcal{Y}} = \boldsymbol{\mathcal{Y}}_{i,j,k}$.

2.2.3) Otherwise, go to Step 2.3, and return to Step 2.2.1.

2.3) Update $\mathcal{W} = \mathcal{W}_{i,j,k}$, $\boldsymbol{\mathcal{X}} = \boldsymbol{\mathcal{X}}_{i,j,k}$, $\boldsymbol{\mathcal{Y}} = \boldsymbol{\mathcal{Y}}_{i,j,k}$ and verify the feasibility of (22b); if this is the case, return to Step 2.

2.4) Otherwise, go to Step 3.

3) Finally, the optimal solution is given by $\mathcal{W}^* = \mathcal{W}_{i,j,k}$, $\boldsymbol{\mathcal{X}}^* = \boldsymbol{\mathcal{X}}_{i,j,k}$, $\boldsymbol{\mathcal{Y}}^* = \boldsymbol{\mathcal{Y}}_{i,j,k}$.

4. Illustrative examples

4.1. Unmanned aerial system trajectory tracking illustrative example. The control action developed in this study is tested on an unmanned aerial vehicle (UAV), such as the one shown in Fig. 1.

The following differential equations serve as a simplified dynamic model of the multi-rotor UAV:

$$\begin{aligned} \ddot{p}_x &= \frac{1}{M}(c_\phi s_\theta c_\psi + s_\phi s_\psi)\bar{u}, \quad \ddot{\phi} = \frac{1}{\mathbb{I}_x}\tau_\phi + \xi_\phi, \\ \ddot{p}_y &= \frac{1}{M}(c_\phi s_\theta s_\psi - s_\phi c_\psi)\bar{u}, \quad \ddot{\theta} = \frac{1}{\mathbb{I}_y}\tau_\theta + \xi_\theta, \\ \ddot{p}_z &= \frac{1}{M}(c_\phi c_\theta)v_1 - g + \xi_z, \quad \ddot{\psi} = \frac{1}{\mathbb{I}_z}\tau_\psi + \xi_\psi, \end{aligned} \tag{24}$$

where the conventional robotic notation $c_* = \cos(*)$, $s_* = \sin(*)$ and $t_* = \tan(*)$ is introduced. The system coordinate determines the inertial frame $\mathcal{I} = \{x_\mathcal{I}, y_\mathcal{I}, z_\mathcal{I}\}$. $\mathcal{B} = \{x_\mathcal{B}, y_\mathcal{B}, z_\mathcal{B}\}$ in East-North-Up (ENU) coordinates, representing the multirotor's body-fixed frame. The position vector of the vehicle's center of mass with respect to $\mathcal{I}$ is denoted by (p_x, p_y, p_z). The

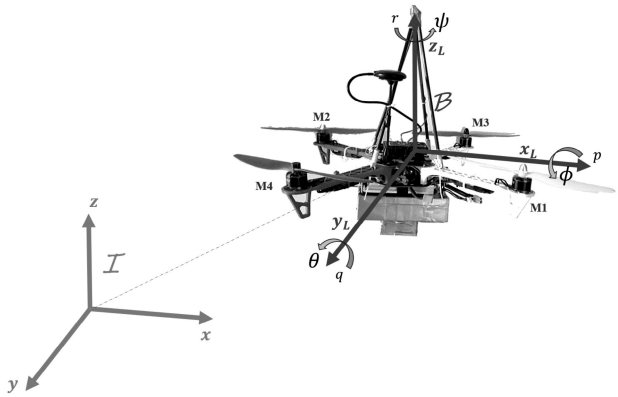

Fig. 1. Multi-rotor unmanned aerial vehicle.

vehicle's orientation vector in terms of roll, pitch, and yaw angles has components ϕ, θ, ψ, respectively. Actually, the corresponding torques for roll, pitch, and yaw are denoted by τ_ϕ, τ_θ, τ_ψ, and the main thrust control input is supplied by $\bar{u}$. The vehicle's mass is denoted by M, the acceleration due to the gravity is defined as g, and the drone moments of inertia are denoted by $\mathbb{I}_x$, $\mathbb{I}_x$, $\mathbb{I}_z$. The disturbance/uncertainty effects with bounded energy on the drone altitude, roll, pitch and yaw torques, are denoted by ξ_z, ξ_ϕ, ξ_θ and ξ_ψ, respectively.

On the assumption that $|\phi| < \pi/2$ and $|\theta| < \pi/2$, consider the stabilization feedback control

$$\bar{u} = \frac{M}{c_\phi c_\theta}\{g + v_1\} \tag{25}$$

and

$$\begin{aligned} \ddot{p}_x &= \left(t_\theta c_\psi + t_\phi \frac{s_\psi}{c_\theta}\right)\{g + v_1\}, \quad \ddot{\phi} = \frac{1}{\mathbb{I}_x}\tau_\phi + \xi_\phi, \\ \ddot{p}_y &= \left(t_\theta s_\psi - t_\phi \frac{c_\psi}{c_\theta}\right)\{g + v_1\}, \quad \ddot{\theta} = \frac{1}{\mathbb{I}_y}\tau_\theta + \xi_\theta, \\ \ddot{p}_z &= v_1 + \xi_z, \qquad \ddot{\psi} = \frac{1}{\mathbb{I}_z}\tau_\psi + \xi_\psi. \end{aligned} \tag{26}$$

Here, the attitude performance of p_x and p_y depends on the angular displacements of θ and ϕ, respectively. In this way, we define the error dynamics performance related to p_x and p_y as

$$\begin{aligned} \dot{\tilde{x}}_1 &= \tilde{x}_2, \quad \dot{\tilde{x}}_2 = -k_1\tilde{x}_1 - k_2\tilde{x}_2, \\ \dot{\tilde{x}}_3 &= \tilde{x}_4, \quad \dot{\tilde{x}}_4 = -k_3\tilde{x}_3 - k_4\tilde{x}_4, \end{aligned} \tag{27}$$

where $\tilde{x}_1 = p_x - p_{xd}$, $\tilde{x}_2 = \dot{p}_x - \dot{p}_{xd}$, $\tilde{x}_3 = p_y - p_{yd}$, $\tilde{x}_4 = \dot{p}_y - \dot{p}_{yd}$ define the position and its velocity error tracking with respect to p_x and p_y. This means that $\dot{\tilde{x}}_2 = \ddot{p}_x - \ddot{p}_{xd}$ and $\dot{\tilde{x}}_4 = \ddot{p}_y - \ddot{p}_{yd}$. As a result, by utilizing both (26) and (27), the following statements are fulfilled:

$$\begin{aligned} -k_1\tilde{x}_1 - k_2\tilde{x}_2 &= \left(t_\theta c_\psi + t_\phi \tfrac{s_\psi}{c_\theta}\right)\{g + v_1\} - \ddot{p}_{xd}, \\ -k_3\tilde{x}_3 - k_4\tilde{x}_4 &= \left(t_\theta s_\psi - t_\phi \tfrac{c_\psi}{c_\theta}\right)\{g + v_1\} - \ddot{p}_{yd}, \end{aligned}$$

where k_1, k_2, k_3 and k_4 are positive constant gains. Isolate θ from the first equation and ϕ from the second one, which yields

$$\theta = \arctan\left(\left\{\frac{-k_1\tilde{x}_1 - k_2\tilde{x}_2 + \ddot{p}_{xd}}{g+v_1} - t_\phi\frac{s_\psi}{c_\theta}\right\}\frac{1}{c_\psi}\right),$$
$$\phi = \arctan\left(\left\{s_\theta s_\psi - \frac{\ddot{p}_{yd} - k_3\tilde{x}_3 - k_4\tilde{x}_4}{g+v_1}\right\}\frac{c_\theta}{c_\psi}\right). \tag{28}$$

It is clear that the yaw angle must always point east. This means that the desired yaw orientation is $\psi_d = 0$, and its velocity $\dot{\psi}_d = 0$. For this case, assume that $|\psi| < \pi/2$. Then, the yaw sub-systems, where $\tilde{x}_{11} = \psi - \psi_d$, $\tilde{x}_{12} = \dot{\psi} - \dot{\psi}_d$, is written as

$$\begin{bmatrix}\dot{\tilde{x}}_{11}\\ \dot{\tilde{x}}_{12}\end{bmatrix} = \begin{bmatrix}0 & 1\\ 0 & 0\end{bmatrix}\begin{bmatrix}\tilde{x}_{11}\\ \tilde{x}_{12}\end{bmatrix} + \begin{bmatrix}0\\ \frac{1}{\mathbb{I}_z}\end{bmatrix}\tau_\psi + \begin{bmatrix}0\\ \xi_\psi\end{bmatrix}, \tag{29}$$

which is in the format (4). Apply Proposition 1 of to considerably reduce the disturbance/uncertain effects on the yaw subsystem. For this case, $\tau_\psi = \boldsymbol{\mathcal{K}}_\psi[\tilde{x}_{11}\ \ \tilde{x}_{12}]^\top$, and its matrix gain is given by

$$\boldsymbol{\mathcal{K}}_\psi = -\mathbb{I}_z\left[\boldsymbol{\mathcal{K}}_{\psi,1},\ \boldsymbol{\mathcal{K}}_{\psi,2}\right], \tag{30}$$
$$\boldsymbol{\mathcal{K}}_{\psi,1} = \mathbf{R}_{\psi,2}^2\mathbf{R}_{\psi,1}, \quad \boldsymbol{\mathcal{K}}_{\psi,2} = \mathbf{R}_{\psi,1} + \mathbf{R}_{\psi,2}.$$

Furthermore, from Assumption 3, we get $\bar{\xi}_{\psi,1} = 0$, and $\bar{\xi}_{\psi,2} = \xi_\psi$, so $\|\bar{\xi}_{\psi,2}\| \le \delta_{\psi,2}$. Actually, the trajectory $\tilde{x}_{11}(t)$ of subsystem (29) is stable in the FTB-sense, with positive fixed scalars $\alpha_{\psi,2}$ and

$$b_{\psi,2} = \sqrt{\frac{\varepsilon_{\psi,2}\delta_{\psi,2}}{\alpha_{\psi,2}}\lambda_{\max}(\mathbf{P}_\psi^{-1})},$$

in finite time

$$T_{\psi,2} = \frac{1}{\alpha_{\psi,2}}\ln\left\{\frac{\alpha_{\psi,2}\lambda_{\max}(\mathbf{P}_\psi)\|z_{01}\|^2 - \beta_2}{\alpha_{\psi,2}\gamma_{\psi,2}}\right\} + T_{\psi,1}$$

for a sufficiently small constant $\gamma_{\psi,2} \in \mathbb{R}^+$. This implies that after finite time $T_{\psi,2}$, the yaw angle is less than $b_{\psi,2}$. In the same way, let us define the p_z sub-systems for robust regulation of the attitude dynamic, where $\tilde{x}_5 = p_z - p_{zd}$, $\tilde{x}_6 = \dot{p}_z - \dot{p}_{zd}$:

$$\begin{bmatrix}\dot{\tilde{x}}_5\\ \dot{\tilde{x}}_6\end{bmatrix} = \begin{bmatrix}0 & 1\\ 0 & 0\end{bmatrix}\begin{bmatrix}\tilde{x}_5\\ \tilde{x}_6\end{bmatrix} + \begin{bmatrix}0\\ 1\end{bmatrix}\tau_\psi + \begin{bmatrix}0\\ \xi_z\end{bmatrix}. \tag{31}$$

which is in the format (4). To significantly lessen the disturbance/uncertain effects on the yaw subsystem, use Proposition 1. For this case, $v_1 = \boldsymbol{\mathcal{K}}_z[\tilde{x}_5\ \ \tilde{x}_6]^\top$, and its matrix gain is given by

$$\boldsymbol{\mathcal{K}}_z = -\left[\boldsymbol{\mathcal{K}}_{z,1},\ \boldsymbol{\mathcal{K}}_{z,2}\right], \tag{32}$$
$$\boldsymbol{\mathcal{K}}_{z,1} = \mathbf{R}_{z,2}^2\mathbf{R}_{z,1}, \quad \boldsymbol{\mathcal{K}}_{z,2} = \mathbf{R}_{z,1} + \mathbf{R}_{z,2}.$$

Assume that the $\bar{\xi}_{z,1} = 0$, and $\bar{\xi}_{z,2} = \xi_\psi$, so $\|\bar{\xi}_{z,2}\| \le \delta_{z,2}$. Actually, the trajectory $\tilde{x}_5(t)$ of subsystem (33) is stable in the FTB-sense, with positive fixed scalars $\alpha_{z,2}$ and

$$b_{z,2} = \sqrt{\frac{\varepsilon_{z,2}\delta_{z,2}}{\alpha_{z,2}}\lambda_{\max}(\mathbf{P}_\psi^{-1})},$$

in finite time

$$T_{z,2} = \frac{1}{\alpha_{z,2}}\ln\left\{\frac{\alpha_{z,2}\lambda_{\max}(\mathbf{P}_z)\|z_{01}\|^2 - \beta_2}{\alpha_{z,2}\gamma_{z,2}}\right\} + T_{z,1}$$

for a sufficiently small constant $\gamma_{z,2} \in \mathbb{R}^+$. This implies that after finite time $T_{z,2}$, the altitude tracking error is less than $b_{z,2}$. As a result of (28), the desired pitch and roll angular displacement may be defined as

$$\theta_d \approx \arctan\left(\frac{-k_1\tilde{x}_1 - k_2\tilde{x}_2 + \ddot{p}_{xd}}{g - \mathbf{R}_{z,2}^2\mathbf{R}_{z,1}\tilde{x}_5 - (\mathbf{R}_{z,1} + \mathbf{R}_{z,2})\tilde{x}_6}\right),$$
$$\phi_d \approx \arctan\left(-\frac{\ddot{p}_{yd} - k_3\tilde{x}_3 - k_4\tilde{x}_4}{g - \mathbf{R}_{z,2}^2\mathbf{R}_{z,1}\tilde{x}_5 - (\mathbf{R}_{z,1} + \mathbf{R}_{z,2})\tilde{x}_6}c_\theta\right). \tag{33}$$

The suggested control strategy is now being employed to stabilize the longitudinal subsystem p_x-θ. The pitch error angle dynamics are defined as

$$\begin{bmatrix}\dot{\tilde{x}}_7\\ \dot{\tilde{x}}_8\end{bmatrix} = \begin{bmatrix}0 & 1\\ 0 & 0\end{bmatrix}\begin{bmatrix}\tilde{x}_7\\ \tilde{x}_8\end{bmatrix} + \begin{bmatrix}0\\ \frac{1}{\mathbb{I}_x}\end{bmatrix}\tau_\theta + \begin{bmatrix}0\\ \xi_\theta\end{bmatrix}, \tag{34}$$

where $\tilde{x}_7 = \theta - \theta_d$, and $\tilde{x}_8 = \dot{\theta} - \dot{\theta}_d$. Here, $\tau_\theta = \boldsymbol{\mathcal{K}}_\theta[\tilde{x}_7\ \ \tilde{x}_8]^\top$, with

$$\begin{aligned}\boldsymbol{\mathcal{K}}_\theta &= -\mathbb{I}_x\left[\boldsymbol{\mathcal{K}}_{\theta,1},\ \boldsymbol{\mathcal{K}}_{\theta,2}\right],\\ \boldsymbol{\mathcal{K}}_{\theta,1} &= \mathbf{R}_{\theta,2}^2\mathbf{R}_{\theta,1},\\ \boldsymbol{\mathcal{K}}_{\theta,2} &= \mathbf{R}_{\theta,1} + \mathbf{R}_{\theta,2}.\end{aligned} \tag{35}$$

As already mentioned, $\bar{\xi}_{\theta,1} = 0$, and $\bar{\xi}_{\theta,2} = \xi_\theta$, so that $\|\bar{\xi}_{\theta,2}\| \le \delta_{\theta,2}$. And the pitch error angle dynamic is stable in the FTB sense, with positive fixed scalar $\alpha_{\theta,2}$ and

$$b_{\theta,2} = \sqrt{\frac{\varepsilon_{\theta,2}\delta_{\theta,2}}{\alpha_{\theta,2}}\lambda_{\max}(\mathbf{P}_\theta^{-1})},$$

in finite time

$$T_{\theta,2} = \frac{1}{\alpha_{\theta,2}}\ln\left\{\frac{\alpha_{\theta,2}\lambda_{\max}(\mathbf{P}_\theta)\|z_{01}\|^2 - \beta_2}{\alpha_{\theta,2}\gamma_{\theta,2}}\right\} + T_{\theta,1},$$

for a sufficiently small constant $\gamma_{\theta,2} \in \mathbb{R}^+$. Similarly, the lateral subsystem p_y-ϕ stabilization may be obtained by considering the roll error angle dynamic as follows:

$$\begin{bmatrix}\dot{\tilde{x}}_9\\ \dot{\tilde{x}}_{10}\end{bmatrix} = \begin{bmatrix}0 & 1\\ 0 & 0\end{bmatrix}\begin{bmatrix}\tilde{x}_9\\ \tilde{x}_{10}\end{bmatrix} + \begin{bmatrix}0\\ \frac{1}{\mathbb{I}_y}\end{bmatrix}\tau_\phi + \begin{bmatrix}0\\ \xi_\phi\end{bmatrix}, \tag{36}$$

Table 1. UAV system parameters.

Description	Notation	Value	Units
UAV mass	M	3.5	kg
Inertia on x frame	$\mathbb{I}_x$	0.01	kg· m^2
Inertia on y frame	$\mathbb{I}_y$	0.01	kg· m^2
Inertia on z frame	$\mathbb{I}_z$	0.01	kg· m^{-2}
Gravity constant	g	9.81	m·s^{-2}

where $\tilde{x}_9 = \phi - \phi_d$, and $\tilde{x}_{10} = \dot{\phi} - \dot{\phi}_d$. Here, $\tau_\phi = \boldsymbol{\mathcal{K}}_\phi[\tilde{x}_9 \;\; \tilde{x}_{10}]^\top$, with

$$\begin{aligned} \boldsymbol{\mathcal{K}}_\phi &= -\mathbb{I}_x\left[\boldsymbol{\mathcal{K}}_{\phi,1},\, \boldsymbol{\mathcal{K}}_{\phi,2}\right], \\ \boldsymbol{\mathcal{K}}_{\phi,1} &= \mathbf{R}_{\phi,2}^2\mathbf{R}_{\phi,1}, \\ \boldsymbol{\mathcal{K}}_{v,2} &= \mathbf{R}_{\phi,1} + \mathbf{R}_{\phi,2}. \end{aligned} \tag{37}$$

As already mentioned, $\bar{\xi}_{\phi,1} = 0$, and $\bar{\xi}_{\phi,2} = \xi_\phi$, so that $\|\bar{\xi}_{\phi,2}\| \le \delta_{\phi,2}$. The pitch error angle dynamic is stable in the FTB-sense, with positive fixed scalars $\alpha_{\phi,2}$ and

$$b_{\phi,2} = \sqrt{\frac{\varepsilon_{\phi,2}\delta_{\phi,2}}{\alpha_{\phi,2}}\lambda_{\max}(\mathbf{P}_\phi^{-1})},$$

in finite time

$$T_{\phi,2} = \frac{1}{\alpha_{\phi,2}}\ln\left\{\frac{\alpha_{\phi,2}\lambda_{\max}(\mathbf{P}_\phi)\|z_{01}\|^2 - \beta_2}{\alpha_{\phi,2}\gamma_{\phi,2}}\right\} + T_{\phi,1},$$

for a sufficiently small constant $\gamma_{\phi,2} \in \mathbb{R}^+$.

For the numerical simulation, the system parameters that were utilized are listed in Table 4.1. A trajectory tracking problem for UAV flying is examined to evaluate our control design. The initial conditions for the UAV are $x_0 = \mathbf{0}_{12}$. To obtain the yaw orientation control action, the following parameters are considered:

$$\|\xi_\psi\| \le 0.5, \quad \alpha_\psi = 30,\ \varepsilon_{1,\psi} = 0.002, \quad \varepsilon_{2,\psi} = 10^{-8}.$$

By using *Yalmip-CVX* Matlab toolboxes, for $R_{1,\psi} = 10$ the numerical procedure presented in Section 3, produces the solution

$$\begin{aligned} R_{2,\psi} &= 15.806, \\ P_\psi &= 2.1907 \times 10^{-8}, \\ Y_\psi &= 7.215 \times 10^8. \end{aligned}$$

This means that the control law for the yaw orientation has the control gain

$$\boldsymbol{\mathcal{K}}_\psi = -\left[1.6037 \;\; 0.2604\right].$$

To implement the altitude controller, the designed feedback control gain use the parameters

$$\|\xi_z\| \le 0.5, \quad \alpha_z = 0.1,$$

$$\varepsilon_{1,z} = 0.0002, \quad \varepsilon_{2,z} = 0.0001.$$

For the considered $R_{1,z} = 10$, the control algorithm yields the solution

$$\begin{aligned} R_{2,z} &= 1.3061, \\ P_z &= 2.1907 \times 10^{-8}, \\ Y_z &= 5.9619 \times 10^7. \end{aligned}$$

Thus, the control gain for the altitude is

$$\boldsymbol{\mathcal{K}}_z = -\left[13.0610 \;\; 11.3061\right].$$

On the other hand, the virtual control gains are selected as $k_1 = 2$, $k_2 = 2.4$, $k_3 = 12$ and $k_4 = 24$. Similarly to the altitude and yaw, control gain subsystems were obtained. For the pitch and yaw subsystem for given $R_{1,\theta} = 10$ and $R_{1,\phi} = 10$, the following parameters are set:

$$\begin{aligned} \|\xi_\theta\| &\le 0.5, & \alpha_\theta &= 30, \\ \varepsilon_{1,\theta} &= 0.002, & \varepsilon_{2,\theta} &= 10^{-6}, \\ R_{2,\theta} &= 15.8061, & P_z &= 2.190 \times 10^{-8}, \\ Y_z &= 7.21 \times 10^8, & \|\xi_\phi\| &\le 0.5, \\ \alpha_\phi &= 3, & \varepsilon_{1,\phi} &= 0.002, \\ \varepsilon_{2,\phi} &= 10^{-7} & R_{2,\phi} &= 2.4732, \\ P_\phi &= 3.1622 \times 10^{-8}, & Y_\phi &= 7.8213 \times 10^7. \end{aligned}$$

Accordingly, the associated control gains are

$$\boldsymbol{\mathcal{K}}_\theta = -\left[1.6037 \;\; 0.2604\right],$$

for the pitch subsystem and

$$\boldsymbol{\mathcal{K}}_\phi = -\left[0.2250 \;\; 0.1225\right],$$

for the roll subsystem.

The numerical example was implemented using Matlab, and a Runge–Kutta method with a fixed step size of 0.001 seconds was utilized. From the parametric circle equation, the UAV's planned trajectory is formed. The goal of using this parametric equation is to minimize the required velocity on the rectangle's vertices. Figure 2 shows the desired position translational coordinates x, y, and z, as well as their closed-loop system response. This figure shows that after time $t = 5$ s, the position P_x arrives at the desired one. Similarly, the position P_y reaches its desired trajectory at time $t = 7$ s. For the altitude position error, the associated ultimate bound is $b_{2,z} = 0.4777$. This means that it starts inside this ball.

The numerical results for the UAV orientation are depicted in Fig. 3. Here, the dashed line defines the desired angular position and the solid line the real one. In this case, the given ultimate bounds for Euler angles

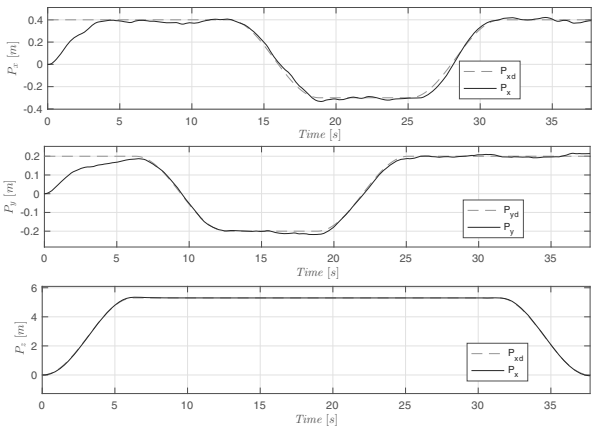

Fig. 2. UAV position in the (x, y, z) frame.

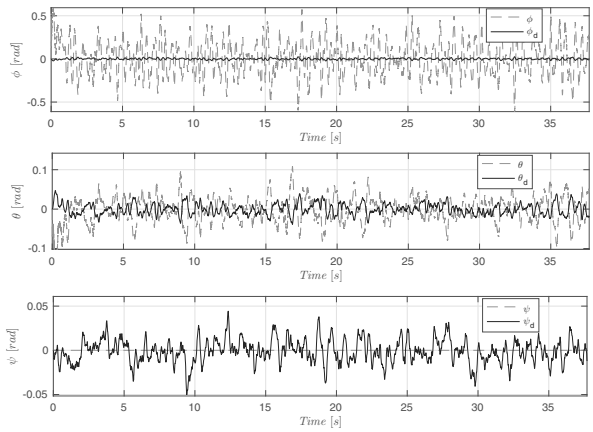

Fig. 3. UAV orientation Euler angles: pitch, yaw and roll.

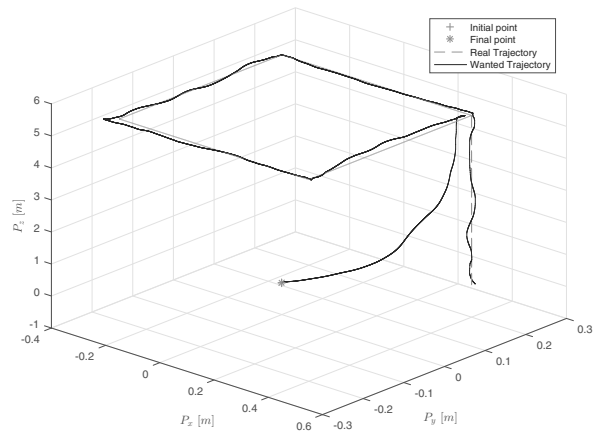

Fig. 4. Drone trajectory flight performance.

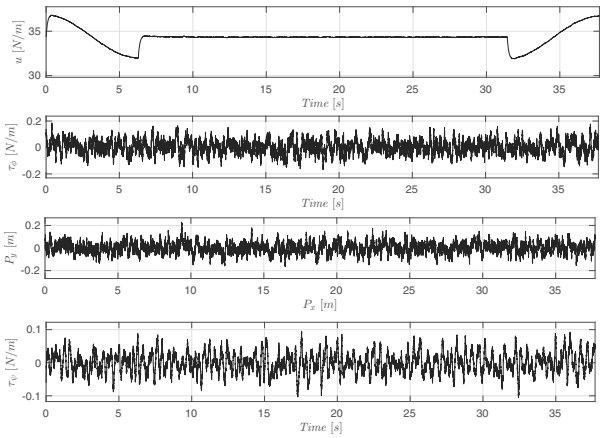

Fig. 5. UAV control signals $\bar{u}$, τ_ϕ, τ_θ and τ_ψ.

are $b_{2,\psi} = 0.0872$, $b_{2,\theta} = 0.0872$ and $b_{2,\phi} = 0.7260$ for the yaw, pitch, and roll angular errors, respectively.

Figure 4 shows the system position performance concerning the designed rectangle trajectory. This numerical result is given by using the designed control action and the system dynamics are under external uncertain disturbances.

Finally, the applied control signal is presented in Fig. 5. This figure contains the thrust input $\bar{u}$, and the associated torques for roll, pitch, and yaw, respectively.

4.2. Benchmark example. Consider the system in the format of (2), where

$$f(x) = \begin{bmatrix} 0.5\sin(x_1 + x_2) \\ -\sin(x_1) + x_2 \end{bmatrix},$$
$$\mathbf{B} = \begin{bmatrix} -1 \\ 1 \end{bmatrix},$$

$$d(t) = \begin{bmatrix} 0.1150\sin(13t - 0.2) \\ -0.3\cos(11.3t + 9.2) \end{bmatrix},$$
$$x(0) = \begin{bmatrix} -2.1 \\ 2.3 \end{bmatrix}, \tag{38}$$
$$\xi_u(t) = -0.1(\sin(20t) + 0.7\cos(19.2t)).$$

Note that the state matrix is defined as

$$\mathbf{A} = \begin{bmatrix} 0.5 & 2 \\ -1 & 1 \end{bmatrix},$$

on the assumption that $x_2 \in (-1, 1)$, $\delta = 8.3024$. Notice that the transformation (3) is not feasible in this case. Therefore, the similarity transformation to a controllable canonical form is applied, where

$$\mathbf{T}^{-1} = \boldsymbol{\mathcal{C}}\mathbf{W}, \quad \mathbf{W} = \begin{bmatrix} 0.5 & 1 \\ 1 & 0 \end{bmatrix}$$

and $\boldsymbol{\mathcal{C}} \in \mathbb{R}^{2\times 2}$ is the controllability matrix. Thus, for the considered parameters $\varepsilon_1 = 2 \times 10^{-11}$, $\varepsilon_2 = \times 10^{-11}$, the

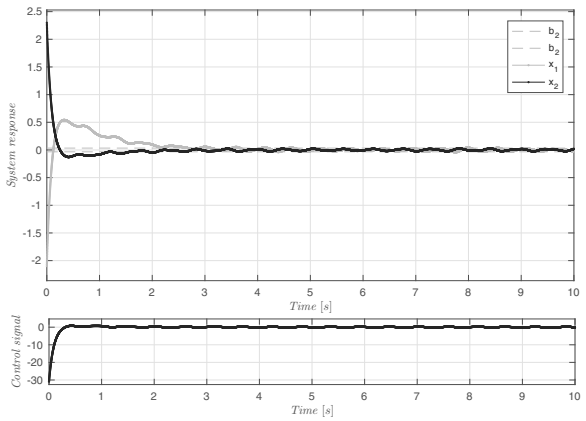

Fig. 6. System response.

numerical procedure presented in Section 3, produces the solution

$$R_2 = 3.75,$$
$$P = 3.7058 \times 10^{-8},$$
$$Y = 1.0119 \times 10^{7}.$$

This means that the control law associated with the yaw orientation has the control gain

$$\mathcal{K} = [-2.3929 \quad -15.6430].$$

Figure 6 depicts the closed loop system response. Notice that, within time $T = 3.95$ s, system trajectories arrive at the ultimate bound of $b_2 = 0.0336$.

5. Conclusions

A robust finite time-bound control was designed to reduce the uncertain dynamics as well as external disturbance effects. To this end, the designed control approach, which is a class of linear feedback control, decouples the effects of matched and unmatched uncertainties and/or external disturbances. In this way, uncertain-disturbance effects can be reduced in a straight forward manner by reducing the effects of unmatched ones by using a constrained matrix inequality problem. Actually, this problem is turned into an optimization problem, which implies a constraint linear matrix inequality problem. Furthermore, theoretical results were validated in numerical simulation over a nonlinear underactuated system.

References

Amato, F., Ambrosino, R., Ariola, M., Cosentino, C., De Tommasi, G. (2014). *Finite-Time Stability and Control*, Springer, London.

Amato, F., Ariola, M., Cosentino, C., Abdallah, C. and Dorato, P. (2003). Necessary and sufficient conditions for finite-time stability of linear systems, *Proceedings of the 2003 American Control Conference, Denver, USA*, Vol. 5, pp. 4452–4456.

Amato, F., Ariola, M. and Dorato, P. (2001). Finite-time control of linear systems subject to parametric uncertainties and disturbances, *Automatica* **37**(9): 1459–1463.

Bhat, S.P. and Bernstein, D.S. (2000). Finite-time stability of continuous autonomous systems, *SIAM Journal on Control and Optimization* **38**(3): 751–766.

Edwards, C. and Spurgeon, S. (1998). *Sliding Mode Control: Theory and Applications*, CRC Press, Boca Raton.

Haddad, W.M. and Chellaboina, V. (2011). *Nonlinear Dynamical Systems and Control: A Lyapunov-based Approach*, Princeton University Press, Princeton.

Khalil, H.K. and Grizzle, J.W. (2002). *Nonlinear Systems*, Vol. 3, Prentice Hall, Upper Saddle River.

Kokotović, P.V., Nicosia, T., Menini, L., Zaccarian, L. and Abdallah, C.T. (2006). *Current Trends in Nonlinear Systems and Control: In Honor of Petar Kokotovic and Turi Nicosia*, Springer, Boston.

Kukurowski, N., Mrugalski, M., Pazera, M. and Witczak, M. (2022). Fault-tolerant tracking control for a non-linear twin-rotor system under ellipsoidal bounding, *International Journal of Applied Mathematics and Computer Science* **32**(2): 171–183, DOI: 10.34768/amcs-2022-0013.

Li, X., Ho, D.W. and Cao, J. (2019). Finite-time stability and settling-time estimation of nonlinear impulsive systems, *Automatica* **99**: 361–368.

Liu, H., Zhong, M. and Yang, R. (2018). Simultaneous disturbance compensation and H_i/H^∞ optimization in fault detection of UAVs, *International Journal of Applied Mathematics and Computer Science* **28**(2): 349–362, DOI: 10.2478/amcs-2018-0026.

Orlov, Y., Aoustin, Y. and Chevallereau, C. (2010). Finite time stabilization of a perturbed double integrator. Part I: Continuous sliding mode-based output feedback synthesis, *IEEE Transactions on Automatic Control* **56**(3): 614–618.

Polyakov, A., Efimov, D. and Perruquetti, W. (2015). Finite-time and fixed-time stabilization: Implicit Lyapunov function approach, *Automatica* **51**: 332–340.

Poznyak, A., Polyakov, A. and Azhmyakov, V. (2014). *Attractive Ellipsoids in Robust Control*, Springer, Cham.

Puangmalai, J., Tongkum, J. and Rojsiraphisal, T. (2020). Finite-time stability criteria of linear system with non-differentiable time-varying delay via new integral inequality, *Mathematics and Computers in Simulation* **171**: 170–186.

Utkin, V.I. and Poznyak, A.S. (2013). Adaptive sliding mode control with application to super-twist algorithm: Equivalent control method, *Automatica* **49**(1): 39–47.

Wang, H., Liu, P.X., Zhao, X. and Liu, X. (2019). Adaptive fuzzy finite-time control of nonlinear systems with actuator faults, *IEEE Transactions on Cybernetics* **50**(5): 1786–1797.

Weiss, L. and Infante, E. (1967). Finite time stability under perturbing forces and on product spaces, *IEEE Transactions on Automatic Control* **12**(1): 54–59.

Yu, S., Yu, X., Shirinzadeh, B. and Man, Z. (2005). Continuous finite-time control for robotic manipulators with terminal sliding mode, *Automatica* **41**(11): 1957–1964.

Patricio Ordaz received his PhD degree in automatic control from CINVESTAV, Mexico City, in 2012. He currently is a professor at the Autonomous University of Hidalgo State. His research interests are in stability analysis of linear and nonlinear systems, optimal control, nonlinear control, robust control, adaptive control, system identification and observation, as well as regulation and stabilization of electromechanical and underactuated systems.

Hussain Alazki received his PhD degree in automatic control from the Center for Research and Advanced Studies of the National Polytechnic Institute, Mexico, in 2011. He is currently a professor at the Mechatronics Department, Autonomous University of Carmen, Campeche, Tabasco. Mexico.

Bonifacio Sánchez received his BEng degree in mechatronics from the Polytechnic University of Pachuca, Pachuca Hidalgo, Mexico, in 2013 and his MSc degree in mechatronics from the same institution in 2015. He is currently on the doctorate program in automatic control from CINVESTAV-IPN, Mexico City, Mexico. He presently works on robust-adaptive nonlinear control, observation and parameters estimation of underactuated electromechanical systems.

Mario Ordaz-Oliver is an electrical engineer, having graduated from Instituto Tecnologico de Pachuca, Hidalgo, Mexico, in 2009. He received his MS in automatic control from the Autonomous University of Hidalgo State, Pachuca de Soto Hidalgo, Mexico, in 2013. He is currently on the doctorate program on automation and control at the same university. His research interests include systems with delays, control systems theory and stability analysis.

Appendix

A1. Proof of Lemma 1

Using

$$\left(\frac{\mathrm{d}}{\mathrm{d}t}V(x(t)) + \alpha V(x(t))\right) e^{\alpha t} = \frac{\mathrm{d}}{\mathrm{d}t} e^{\alpha t} V(x(t)), \quad \text{(A1)}$$

and multiplying both sides of (7) by $e^{\alpha t}$, we get the differential inequality

$$\frac{\mathrm{d}}{\mathrm{d}t} e^{\alpha t} V(x(t)) \le \beta e^{\alpha t} \sqrt{V(x(t))}. \quad \text{(A2)}$$

The solution of the equation

$$\int_{t_0}^{t} \frac{\frac{\mathrm{d}}{\mathrm{d}s} e^{\alpha s} V(x(s))}{\sqrt{e^{\alpha s} V(x(s))}} \mathrm{d}s = \beta \int_{t_0}^{t} e^{\frac{1}{2}\alpha s} \mathrm{d}s, \quad \text{(A3)}$$

yields

$$e^{\frac{\alpha}{2}s} V^{\frac{1}{2}}(x(s))\Big|_{t_0}^{t} = \frac{\beta}{\alpha} \exp\left(\frac{1}{2}\alpha s\right)\Big|_{t_0}^{t}. \quad \text{(A4)}$$

From the comparison principle (see, e.g., Haddad and Chellaboina, 2011; Khalil and Grizzle, 2002), the solution of (A3) satisfies the differential inequality (7) since

$$V^{\frac{1}{2}}(t) \le \frac{2\beta}{\alpha} + e^{-\alpha(t-t_0)} \left\{ V^{\frac{1}{2}}(t_0) - \frac{2\beta}{\alpha} \right\}. \quad \text{(A5)}$$

This means that

$$\lim_{t\to\infty} \sqrt{V(t)} \le \frac{2\beta}{\alpha}.$$

Thus, for a sufficiently large α such that $\alpha > 2\beta$, we have $\lim_{t\to\infty} \sqrt{V(t)} \le \mu$, with $0 < \mu < 1$, for some $\mu = 2\beta/\alpha + \gamma$. Actually, from (A5), for the case when the initial condition $V(t_0)$ is less than μ^2, the trajectory $V(t)$ remains in a vicinity of ratio μ for all times $t \ge t_0$. Otherwise, when $V(t_0)$ is greater than μ^2, the function $V(t)$ is decreasing. This means that, since time t is increasing, the function arrives into a vicinity around the origin in finite time (8). Even more, the trajectory $V(t)$ remains on it for all future times $T \ge t_r$ and the lemma is proven.

A2. Proof of Lemma 2

For the upper bound of (9) and premultiplying by $e^{\alpha t}$, note that the solution of differential equation

$$e^{\alpha t} \left\{ \frac{\mathrm{d}}{\mathrm{d}t} V(t) + \alpha V(t) \right\} = \beta e^{\alpha t} \quad \text{(A6)}$$

along the time interval $s \in [t_0, t]$ yields

$$V_2(t) = \frac{\beta}{\alpha} + \left\{ V_2(t_0) - \frac{\beta}{\alpha} \right\} e^{-\alpha(t-t_0)}.$$

By the comparison principle, the solution of the differential equation (A6) refers to the solution of (9) as

$$V(t) \le \frac{\beta}{\alpha} + \left\{ V(t_0) - \frac{\beta}{\alpha} \right\} e^{-\alpha(t-t_r)}. \quad \text{(A7)}$$

The previous differential inequality solution directly concludes with (10), implying that Definition 1 is fulfilled. Moreover, the storage function $V_2(t)$ is an attractive invariant set, and the Lemma is proven.

A3. Proof of Proposition 1

Let the storage function $V_1(\varphi) = \frac{1}{2}\varphi^\intercal\varphi$, with its time derivative given as follows:

$$\begin{aligned}\frac{\mathrm{d}}{\mathrm{d}t}V_1(\top) &= \varphi^\intercal\left(\bar{\mathbf{H}}_1 z_1 + \bar{\mathbf{H}}_1 z_2 + \bar{\xi}_2 + \mathbf{R}_1\bar{\xi}_1 + \boldsymbol{\mathcal{B}}_2 u\right),\\ \bar{\mathbf{H}}_1 &= \boldsymbol{\mathcal{A}}_{21} + \mathbf{R}_1\boldsymbol{\mathcal{A}}_{11},\\ \bar{\mathbf{H}}_2 &= \boldsymbol{\mathcal{A}}_{22} + \mathbf{R}_1\boldsymbol{\mathcal{A}}_{12}.\end{aligned} \tag{A8}$$

Selecting the control law $u = u_1 + u_2$, where

$$u_1 = -\boldsymbol{\mathcal{B}}_2^{-1}\left(\bar{\mathbf{H}}_1 z_1 + \bar{\mathbf{H}}_1 z_2\right), \tag{A9}$$

the time derivative of the storage function is

$$\frac{\mathrm{d}}{\mathrm{d}t}V_1(\top) = \varphi^\top\bar{\xi}_2 + \varphi^\top\mathbf{R}_1\bar{\xi}_1 + \varphi^\top\boldsymbol{\mathcal{B}}_2 u. \tag{A10}$$

From this differential equation, we get:

$$\begin{aligned}&\bar{\xi}_2 + \varphi^\top\mathbf{R}_1\bar{\xi}_1 + \varphi^\top\boldsymbol{\mathcal{B}}_2 u\\ &\qquad \le |\varphi^\top\bar{\xi}_2 + \varphi^\top\mathbf{R}_1\bar{\xi}_1| + \varphi^\top\boldsymbol{\mathcal{B}}_2 u.\end{aligned} \tag{A11}$$

Then, by the Cauchy–Schwartz inequality,

$$\|\varphi^\top\bar{\xi}_2 + \varphi^\top\mathbf{R}_1\bar{\xi}_1\| \le \sqrt{2\varphi^\top\varphi}\sqrt{\xi_1^\top\mathbf{R}_1^\top\mathbf{R}_1\xi + \xi_2^\top\xi_2}. \tag{A12}$$

Since $\mathbf{R}_1^\top\mathbf{R}_1$ is a symmetric matrix, using the Rayleigh–Ritz majorization and Assumption 3, it is evident that

$$\begin{aligned}\xi_1^\top\mathbf{R}_1^\top\mathbf{R}_1\xi &\le \lambda_{\max}(\mathbf{R}_1^\top\mathbf{R}_1)\xi_1^\top\xi_1\\ &= \lambda_{\max}(\mathbf{R}_1^\top\mathbf{R}_1)\delta_1.\end{aligned} \tag{A13}$$

Therefore,

$$\frac{\mathrm{d}}{\mathrm{d}t}V_1(\varphi) \le \beta_1\sqrt{V_1(\varphi)} + \varphi^\top\boldsymbol{\mathcal{B}}_2 u. \tag{A14}$$

Now, using the controller

$$u_2 = -\mathcal{B}_2^{-1}\mathbf{R}_2\varphi, \tag{A15}$$

where $\mathbf{R}_2 \in \mathbb{R}^{m\times m}$ is a diagonal positive definite matrix gain, the previous differential inequality yields

$$\frac{\mathrm{d}}{\mathrm{d}t}V_1(\varphi) \le \beta_1\sqrt{V_1(\varphi)} - \varphi^\top\mathbf{R}_2\varphi. \tag{A16}$$

Again, from the Rayleigh–Ritz quotient we get $\lambda_{\min}(\mathbf{R}_2)\varphi^\top\varphi \le \varphi^\top\mathbf{R}_2\varphi \le \lambda_{\max}(\mathbf{R}_2)\varphi^\top\varphi$. This implies that Lemma 1 is satisfied for $\alpha_1 = 2\lambda_{\min}(\mathbf{R}_2)$. Furthermore, from (A5) and using the fact that $\|\varphi\| = \sqrt{2}V_1^{\frac{1}{2}}(\varphi)$, we have

$$\|\varphi\| \le \frac{\sqrt{2}\beta_1}{\alpha_1} + e^{-\alpha_1(t-t_0)}\left\{\|\varphi_0\| - \frac{\sqrt{2}\beta_1}{\alpha_1}\right\}, \tag{A17}$$

which implies that the trajectory φ arrives in a finite time (13) to the attractive set Ω_1. Finally, $u = u_1 + u_2$ is given from (A9)–(A15) and the result follows.

A4. Proof of Proposition 2

Consider the storage function $V_2(z_1) = z_1^\top\mathbf{P}z_1$, with a symmetric positive definite matrix $\mathbf{P} \in \mathbb{R}^{(n-m)\times(n-m)}$ associated with system (15). The time derivative of the storage function $V_2(z_1)$ along the trajectories (16) is

$$\begin{aligned}&\frac{\mathrm{d}}{\mathrm{d}t}V_2(z_1)\\ &= \begin{bmatrix} z_1\\ \bar{\xi}_1\\ \varphi\end{bmatrix}^\top \begin{bmatrix}\mathbf{PF} + \mathbf{F}^\intercal\mathbf{P} + \alpha_2\mathbf{P} & \mathbf{P} & \mathbf{P}\mathcal{A}_{12}\\ \mathbf{P} & \mathbf{0} & \mathbf{0}\\ \mathcal{A}_{12}^\intercal\mathbf{P} & \mathbf{0} & \mathbf{0}\end{bmatrix}\begin{bmatrix} z_1\\ \bar{\xi}_1\\ \varphi\end{bmatrix}.\end{aligned} \tag{A18}$$

By adding and subtracting the terms $\alpha_2 V_2(z_1)$, $\varepsilon_1\|\bar{\xi}_1\|^2$ and $\varepsilon_2\|\varphi\|^2$, for positive constant scalars α, ε_1 and ε_2, we get

$$\begin{aligned}\frac{\mathrm{d}}{\mathrm{d}t}V_2(z_1) &= \begin{bmatrix} z_1\\ \bar{\xi}_1\\ \varphi\end{bmatrix}^\intercal \mathbf{W}\begin{bmatrix} z_1\\ \bar{\xi}_1\\ \varphi\end{bmatrix}\\ &\quad - \alpha_2 V_2(z_1) + \varepsilon_1\|\bar{\xi}_1\|^2 + \varepsilon_2\|\varphi\|^2.\end{aligned} \tag{A19}$$

From Assumption 3, if the matrix $\mathbf{W}$ is negative definite, we deduce that

$$\frac{\mathrm{d}}{\mathrm{d}t}V_2(z_1) \le -\alpha_2 V_2(z_1) + \beta_2. \tag{A20}$$

Applying Lemma 2, the finite time bound stability is concluded. The solution of the previous inequality is given by

$$V_2(z_1) \le \frac{\beta_2}{\alpha_2} + \left\{V(z_1(T_1)) - \frac{\beta_2}{\alpha_2}\right\}e^{-\alpha_2(t-T_1)}, \tag{A21}$$

which leads to (18), and the proposition is proven.

A5. Proof of Corollary 8

From Proposition 1 and (15), notice that

$$\begin{aligned}\|z_2\| &= \|\varphi - \mathbf{R}_1 z_1\|\\ &\le \|\varphi\| + \|\mathbf{R}_1 z_1\|\\ &\le \frac{\sqrt{2}\beta_1}{\alpha_1} + \gamma_1 + \|\mathbf{R}_1 z_1\|\\ &\le \frac{\sqrt{2}\beta_1}{\alpha_1} + \gamma_1 + \sqrt{\lambda_{\min}(\mathbf{R}_1^\intercal\mathbf{R}_1)}\|z_1\|\end{aligned} \tag{A22}$$

and using Proposition (2), the system trajectory z_1 is TFB stable, with bound

$$b_2 = \sqrt{\frac{\beta_2}{\alpha_2}\lambda_{\max}(\mathbf{P^{-1}})},$$

and finite time T_2. Then

$$\begin{aligned}\|z_2\| &\le \frac{\sqrt{2}\beta_1}{\alpha_1} + \gamma_1\\ &\quad + \sqrt{\frac{\beta_2}{\alpha_2}\lambda_{\min}(\mathbf{R}_1^\intercal\mathbf{R}_1)\lambda_{\max}(\mathbf{P^{-1}})}.\end{aligned} \tag{A23}$$

Furthermore, since $\|z\| = \sqrt{\|z_1\|^2 + \|z_2\|^2}$, using the transformation invariance property $z = \mathbf{T}x$, we get $\|x\| = \|\mathbf{T}^{-1}z\| \leq \sqrt{\lambda_{\max}(\mathbf{T}^{-1})}\|z\|$. Then (20) is concluded, and the result follows.

A6. Proof of Lemma 3

Consider the matrix

$$\mathbf{G} = \begin{bmatrix} \mathbf{P}^{-1} & \mathbf{0} & \mathbf{0} \\ \mathbf{0} & \mathbf{I} & \mathbf{0} \\ \mathbf{0} & \mathbf{0} & \mathbf{I} \end{bmatrix},$$

as a matrix transformation $\mathbf{G}^\top\mathbf{W}\mathbf{G}$. If $-\mathbf{W}$ is a positive definite matrix, then the transformation $\mathbf{G}^\top\mathbf{W}\mathbf{G}$ results in a positive definite matrix. Next, from $\mathbf{G}^\intercal\mathbf{W}\mathbf{G}$, select $\mathbf{X} = \mathbf{P}^{-1}$ and $\mathbf{Y} = \mathbf{R}_1\mathbf{X}$, and $\mathcal{W}$ is obtained.

Received: 27 March 2022
Revised: 8 July 2022
Re-revised: 20 September 2022
Accepted: 21 September 2022